Magnetization and magnetic anisotropy energy of ultrathin Fe films on GaAs(001) exposed to oxygen

2006 J. Phys.: Condens. Matter 18 8791

(http://iopscience.iop.org/0953-8984/18/39/010)

INSTITUTE OF PHYSICS PUBLISHING JOURNAL OF PHYSICS: CONDENSED MATTER

J. Phys.: Condens. Matter **18** (2006) 8791–8802 doi:10.1088/0953-8984/18/39/010

Magnetization and magnetic anisotropy energy of ultrathin Fe films on GaAs(001) exposed to oxygen

Th Kebe, Kh Zakeri, J Lindner, M Spasova and M Farle

Fachbereich Physik, Experimentalphysik-AG Farle, Universität Duisburg-Essen, Lotharstraße 1, 47048 Duisburg, Germany

E-mail: tkebe@agfarle.uni-duisburg.de

Received 24 April 2006, in final form 7 August 2006
Published 11 September 2006
Online at stacks.iop.org/JPhysCM/18/8791

Abstract

The remanent magnetization and the magnetic anisotropy energy of 5–16 monolayer (ML) epitaxial Fe films grown on GaAs(001) were quantitatively monitored *in situ* by superconducting quantum interference device magnetometry and ferromagnetic resonance as a function of oxygen exposure at 300 K. We find that at an oxygen dose of 10 L the perpendicular uniaxial anisotropy $K_{2\perp}$ decreases by almost 50%, whereas the magnetization is decreased by 8% only in the case of a 5 ML Fe film. The fourfold anisotropy constant K_4 and in-plane uniaxial anisotropy constant $K_{2\parallel}$, however, remain unchanged. Low-energy electron diffraction spots of the Fe surface disappear after 6 L of oxygen, indicating a disordered Fe oxide growth. For exposures below 70 L we observe a reduction of the remanent magnetization irrespective of the film thickness. At exposures >70 L we find a faster decrease of the remanent magnetization for the thinner films which is attributed to the finite size effect and a thickness dependent surface roughness of the iron films, respectively. As evidenced by Auger electron spectroscopy and x-ray diffraction, the iron oxide is found to be FeO in the first stage of oxidation, transforming into γ-Fe_2O_3 at higher dosages (>1000 L).

1. Introduction

The oxidation of iron surfaces has been a subject of intense research for several decades [1]. Fe oxide films have been selectively prepared by various methods including, for example, growth of Fe_3O_4 films using sputter deposition from iron oxide targets [2] or co-deposition of Fe in an atomic oxygen atmosphere [3] including a post-annealing procedure. Fe_2O_3 films of greater thickness ranging from 80 to 520 nm were fabricated using pulsed laser deposition (PLD) [4]. Most of the studies dealt with the question of how Fe surfaces are oxidized as a function of oxygen exposure and temperature and focused on structural, chemical and electronic properties [5–7]. *Ab initio* calculations on a Fe(001) surface by Bloński *et al*

predicted a preferred oxygen adsorption at the fourfold hollow sites on the (001) surface at an oxygen coverage of 1/4 monolayers (ML) which also corresponds to the c(2 × 2) reconstruction [8] observed by low-energy electron diffraction (LEED) [9]. In the literature there exist contradictory results on the formation of the Fe(001)c(2 × 2)-O superstructure in LEED imaging during the initial step of chemisorption of oxygen [10]. The incorporation of O into the Fe film has been observed at exposures of 3 and 20 L [7].

Only a little experimental work has been done on the influence of oxygen dosage on the *magnetic parameters* of Fe films. Bloński *et al* [8] predicted that the presence of oxygen can increase the magnetic moment of Fe atoms in the topmost layer by up to 25% and to some extent can even increase the magnetic moments of the Fe layers underneath. The degree of increase of the magnetic moments depends on the sites of the oxygen on or in the Fe film. Salvietti *et al* found by spin polarized He^* de-excitation spectroscopy that above 3–4 L oxygen an oxide surface layer is formed which is magnetically inactive since the asymmetry of the spin-selected density of states vanishes [11]. Using conversion Mössbauer spectroscopy (CEMS) a spin-glass-like frustrated state of the magnetic moments in a thin oxide layer was observed [12] which was obtained by exposure of Fe in air. The reason for the absence of work on magnetic data stems from the fact that quantitative measurements of the magnetization and the magnetic anisotropy require the preparation of thin Fe films on a non-ferromagnetic substrate and *in situ* magnetic characterization techniques. Getzlaff *et al*, who employed angle and spin resolved photoelectron spectroscopy on Fe(110) films exposed to oxygen, found an exchange splitting of the O $2p_x$ level which indicates a magnetic coupling between the chemisorbed oxygen and the Fe layer [13]. However, these measurements only indirectly probe the magnetic moments and did not yield magnetic information above 15 L oxygen. The current work presents a detailed study of the evolution of the remanent magnetization by measuring the magnetic stray field of the *whole* magnetic film and the magnetic anisotropy of lattice distorted Fe monolayers on GaAs(001) exposed to oxygen at exposures up to 25 000 L.

2. Experimental details

The experiments were carried out in a UHV chamber at a base pressure of 2×10^{-10} mbar. Prior to Fe deposition the GaAs(001) substrate was heated to 600 °C and sputtered by Ar ions at 500 eV, target current $I_t = 5\ \mu$A and Ar pressure $p_{Ar} = 1 \times 10^{-5}$ mbar for 30 min. This results in a clean 4 × 6 reconstructed surface [14] characteristic of a flat Ga rich surface which was confirmed by low-energy electron diffraction (LEED). After cooling down to room temperature, Auger electron spectroscopy (AES) did not show any residual C or O. Fe films were grown by e-beam evaporation at pressures below 10^{-9} mbar at 300 K and evaporation rates of 1 ML Fe (=1.43 Å) per minute. AES reveals Fe surfaces with only traces of O corresponding to a coverage below 0.1 ML. Our UHV system is also equipped with facilities for *in situ* scanning superconducting quantum interference device (SQUID) magnetometry [15] and *in situ* ferromagnetic resonance (FMR). A quartz microbalance was used for measuring the thickness of the deposited Fe films. Structural effects of the Fe oxide formation were studied using LEED and Intensity/Voltage (IV) LEED.

In order to find the absolute values of the sample magnetization M the z-component of the magnetic stray field was recorded as a function of position x and y at a height h above the Fe film with a SQUID sensor [15]. The films were magnetically saturated along the easy axis. The easy axis of magnetization of thin Fe films on GaAs is oriented along the [1 1 0] direction due to a large uniaxial in-plane anisotropy originating from the Fe/GaAs interface [16]. We oriented the GaAs substrate such that the [1 1 0] direction coincides with the scanning direction of the SQUID (denoted as the x direction in figure 1). A qualitative

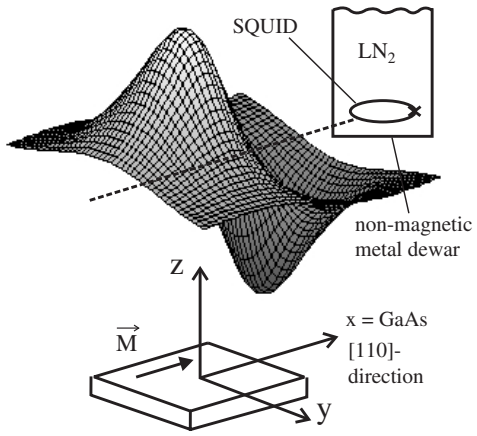

Figure 1. Schematics of the *in situ* SQUID setup. The magnetic stray field component B_z for a ferromagnetic film with the magnetization directed along the x-axis is shown at a fixed height $z \approx h$. The sample is scanned along x.

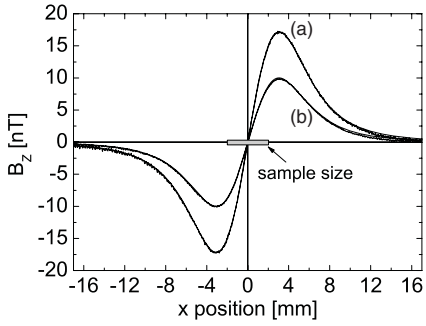

Figure 2. Magnetic stray field component B_z as a function of position x (at $y = 0$) for an 8 ML Fe film on GaAs(001) before (a) and after exposure to 504 L oxygen (b) at 300 K. Fits according to equation (A.1) are plotted together with the experimental data.

sketch of the distribution of the z-component of the sample stray field in the x, y-plane is added, plotted for a typical distance h of the SQUID sensor from the saturated Fe film. The stray field of a homogenously in-plane magnetized film of square shape has been calculated analytically. The analytical solution for the z-component of the stray field can be found in the appendix. By fitting the analytical expression for the magnetic field to the experimental data the sample magnetization was deduced absolutely. Figure 2 shows two line scans across the centre of an 8 ML Fe film before and after oxidation with 504 L O_2. From the magnitude of the magnetization M measured without oxygen, which equals the Fe bulk value within the error bar, we conclude that the sample is in a homogenously magnetized single domain state. The uncertainty of the absolute magnetization determination is below 5% whereas the relative deviation during oxidation steps is below 1%. All films under investigation, including a 5, 8 and 16 ML Fe film, showed an in-plane easy axis of magnetization along [1 1 0], which means that even for the 16 ML film no in-plane reorientation of the easy axis of magnetization along the [100] direction took place in accordance with [17].

Angular dependent *in situ* FMR measurements are performed in the same apparatus as described earlier [18]. The measurements were carried out at $f = 4$ and 9 GHz with the

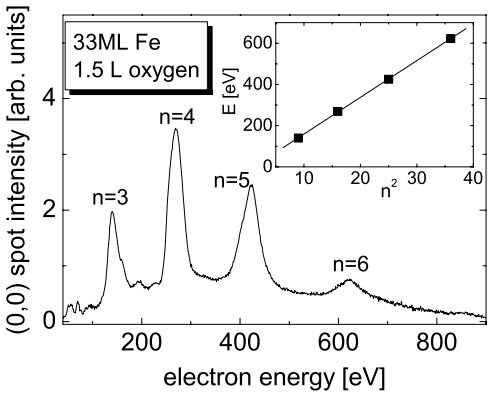

Figure 3. Intensity of the central (0, 0) LEED spot as a function of primary electron energy. The inset shows the peak energies versus square of the order of Bragg reflection. The slope of the linear fit is used to determine the vertical interlayer distance d.

external magnetic field applied along the in-plane [1 $\bar{1}$ 0] direction with respect to the GaAs substrate. Anisotropy constants were determined from polar angle dependences within the ([1 $\bar{1}$ 0], z) plane, z being the film normal, as described in detail in [16] for example. Pure oxygen (99.998 vol%) was dosed in exposure steps of 200 s with pressures ranging from 5×10^{-9} to 5×10^{-5} mbar.

3. Experimental results and discussion

Formation of Fe oxides is accompanied by a change of the lattice parameter, since oxygen atoms have a greater ionic diameter than Fe atoms and ions. We studied the vertical inter layer spacing during the Fe oxide formation by IV-LEED. A typical IV-LEED spectrum is shown in figure 3. The lowest order Bragg peak to be evaluated is $E = 140$ eV ($n = 3$). For high-energy electrons the influence of the inner potential V is negligible, and the band structure approaches that of free electrons. In figure 3 small peaks at $E = 55$, 70, 96, 196 and 229 eV which are not Bragg peaks arise from multiple scattering and are therefore not taken into consideration. Analysing the slope of E over n^2 (inset of figure 3) according to [25] we determine the vertical interlayer distance d. For various oxygen doses on a 33 ML Fe film at room temperature we were able to carry out the measurements up to oxygen exposures above 50 L. Beyond this dose diffraction spots become very diffuse, and the analysis of IV-LEED spectra is no longer possible. We observed at all film thicknesses that an oxygen exposure of 6 L destroys the LEED pattern of the Fe(001) surface. Nevertheless the intensity variation upon variation of the electron energy can even be observed at higher exposures which can be understood from the larger penetration depth of the electrons at higher energies. Figure 4 shows the averaged interlayer distance at successive oxidation steps. Without exposing the film to oxygen we observe an increased interlayer distance as compared to Fe bulk, which is explained by the epitaxial growth of Fe ($a = 2.866$ Å) on GaAs(001) ($a = 5.653$ Å) [27]. The lateral isotropic lattice compression of 1.4% causes the increase of the vertical interlayer distance by 2.2% ($d_{\text{inter}}^{33\,\text{ML Fe}} = 1.464 \pm 0.005$ Å) compared to the α-Fe bulk value ($d_{\text{inter}}^{\text{bulk Fe}} = 1.433$ Å) for the measured 33 ML Fe film. A thickness dependent measurement of the vertical interlayer distance (not presented here) shows an increased interlayer distance of about 3% up to a Fe thickness of 20 ML. Above this thickness the interlayer spacing decreases again. Filipe *et al* [26] found that the vertical lattice constant relaxes towards its bulk value at a Fe thickness of

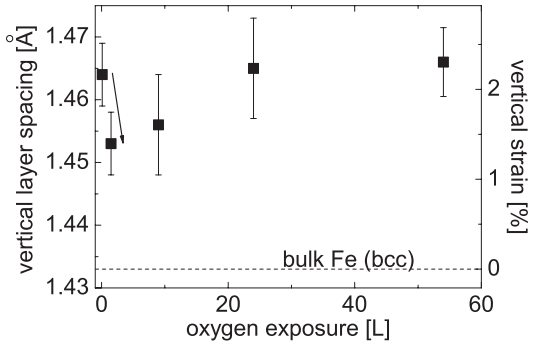

Figure 4. The change of the averaged vertical layer spacing d of the topmost Fe layers during oxygen exposure derived from IV-LEED measurements.

about 160 ML. After an initial dose of only 1.5 L oxygen we find a decrease in the vertical lattice constant of about 0.7%. This corresponds to a decrease of vertical strain of more than 30% which may be attributed to a charge transfer from the Fe atoms to the chemisorbed oxygen. With increasing oxygen exposure one again finds an enlargement of the interlayer distance, since now Fe oxides are formed and all Fe oxides have a greater interlayer distance along their principal [0 0 1] direction in comparison to α-Fe, e.g. $d_{\mathrm{inter}}^{\mathrm{FeO}} = 2.166$ Å and $d_{\mathrm{inter}}^{\gamma-\mathrm{Fe_2O_3}} = 2.0805$ Å. It will be shown later that the Fe oxide thickness will not exceed 2 ML for a dosage up to 50 L oxygen. Thus, one should note that due to the exponentially damped penetration depth of the electrons part of the underlying Fe film is probed as well and an averaged interlayer distance is observed that is smaller than that of the oxides. At the initial stage of oxidation we performed online monitoring of the LEED image of a 33 ML Fe/GaAs(001) film up to exposures of 1.5 L oxygen. Line scans along the [1 0 0] direction as shown in figure 5(a) reveal a weak extra LEED spot in between the $(\bar{1}, 1)$ and (1, 1) LEED spots. The two high intensities shown originate from the cubic symmetry of the Fe(001) surface. The middle section of the line scan is expanded by a factor of five for a better illustration, and clearly indicates an extra spot according to a c(2 × 2) superstructure. However, the intensity is only about 5% of the $(\bar{1}, 1)$ spot intensity and vanishes at about 1 L of oxygen exposure, which indicates structural disorder of the superstructure.

To get an insight into the composition of the iron oxide, Auger spectroscopy measurements of the low-energy transitions have been performed on a 33 ML Fe film. Figure 5(b) shows $M_{2,3}$VV Auger spectra of Fe films for various oxygen doses. A contamination-free Fe film exhibits a distinct peak at 46.5 eV. At only 1.5 L oxygen, which according to [7] corresponds to an oxygen coverage of approximately 0.25 ML, the Fe Auger peak shows characteristic features [20] of FeO. This is consistent with scanning tunnelling microscopy (STM) investigations on a Fe(110) surface at low oxygen coverage from above 0.25 ML also indicating the formation of FeO [28]. At exposures above 1000 L the Auger line shape shows two clear minima at 43 and 51.5 eV which is characteristic for Fe_2O_3 [21]. There exist two modifications of Fe_2O_3, haematite (α-Fe_2O_3), which is an antiferromagnet, and the ferrimagnet maghemite (γ-Fe_2O_3), which has a saturation magnetization of $M = 371 \pm 27$ kA m^{-1} at room temperature (RT) [29]. To decide which modification of Fe_2O_3 is formed, a 20 ML Fe film was prepared in UHV and exposed to ambient conditions. X-ray diffraction (XRD) measurements performed on this film show that after exposure to air polycrystalline γ-Fe_2O_3 is formed. It should be noted that from XRD measurements alone, it is hard to decide whether γ-Fe_2O_3 or Fe_3O_4 is present, since both oxides have an inverse spinel structure with almost the same lattice

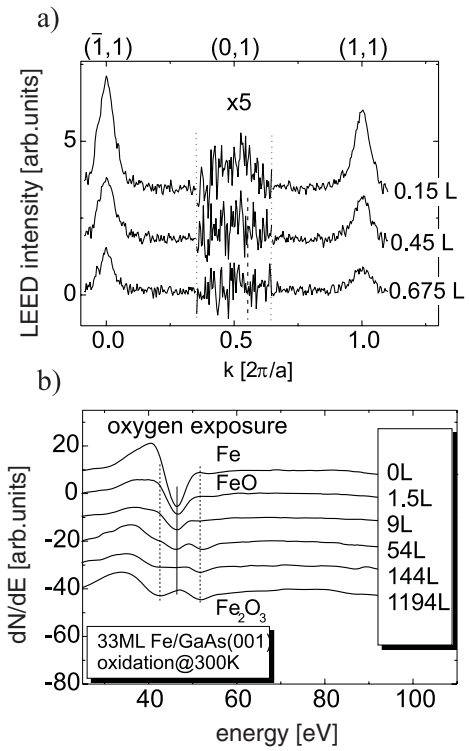

Figure 5. (a) Intensity line scan along the [1 1 0] direction across the ($\bar{1}$, 1) and (1, 1) LEED spot for oxygen exposures of 0.15, 0.45 and 0.675 L. (b) Evolution of the $L_{2,3}VV$ Auger transition for different oxygen exposure steps measured on a 33 ML Fe film at room temperature.

constant. The combination of AES and XRD measurements leads us to the conclusion that high oxygen exposure of thin Fe/GaAs films results in polycrystalline γ-Fe_2O_3. In contrast to the XRD results obtained for a film with a thick oxide layer, the LEED investigation with vanishing LEED spots shows a strong disorder after low exposures below 10 L within the transfer width t of the LEED optics, which is typically of the order of 100 Å. That means that if crystallites develop at low exposures they must be smaller than t.

From the magnitude of the remanent magnetization at RT, which equals the Fe bulk value for all investigated film thicknesses, we conclude that no magnetic dead layers are present at the Fe–GaAs interface. Figure 6(a) shows the changes of the remanent magnetization M of an 8 ML Fe film as a function of oxygen exposure at 300 K. The decrease of the magnetization is fastest at lower exposures, whereas the progress of oxidation slows down at higher values and seems to approach a constant value. Figure 6(b) shows the remanent magnetization of three different films with thicknesses of 5, 8 and 16 ML on a logarithmic scale. To show the reproducibility of our measurements the 8 ML Fe film was measured twice. Each measurement can be divided into two sections with different slopes. Below 100 L the decrease on the logarithmic scale is much slower than it is at higher exposures. In the logarithmic plot the negative slope is steeper the thinner the Fe film is.

The 5 ML Fe film at 300 K loses its remanent magnetization already at 300 L. After the remanence vanished we saturated the film again in a magnetic field but it still showed no remanence. The 8 ML (16 ML) film on the other hand still retains 19% (75%) of the

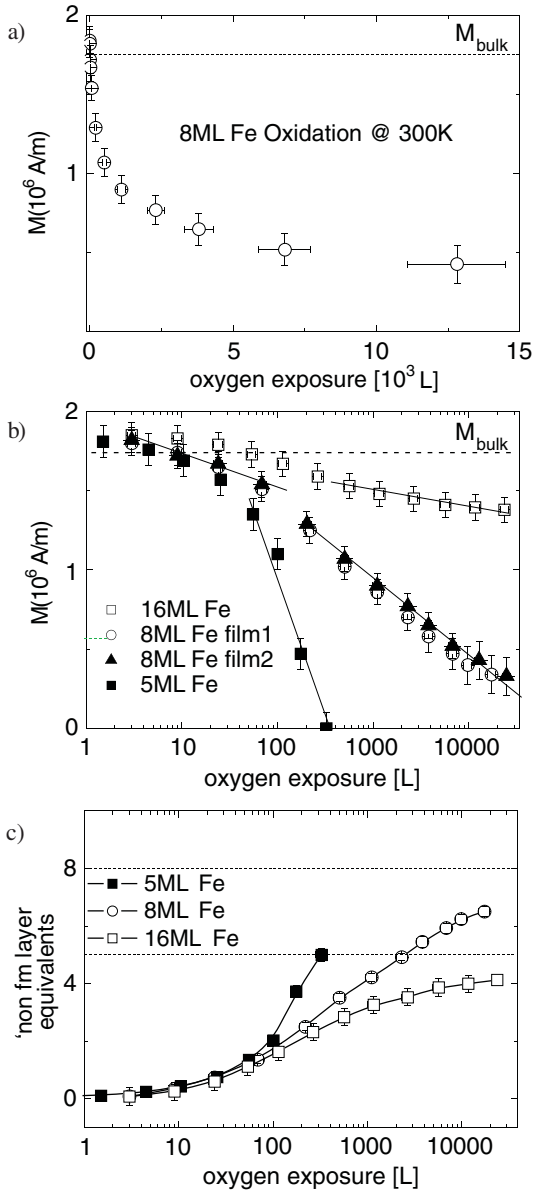

Figure 6. (a) Remanent magnetization M derived as a function of oxygen exposure for a 8 ML Fe film on GaAs(001). (b) Remanent magnetization during successive RT oxidation steps for 5, 8 and 16 ML Fe. All measurements were performed at 300 K. (c) Plot of non-ferromagnetic (fm) layers as a function of oxygen exposures. The values have been calculated from magnetization data of (b) taking into consideration the individual film thicknesses.

initial magnetization value at 300 L. The influence of oxygen on the thicker films seems less, but since magnetization is defined as magnetic moment per volume one has to consider the thickness of the films. Consequently, we calculated the number of oxidized layers under the premise that oxidized Fe does not contribute to the remanent magnetization (see figure 6(c)). This assumption is supported by the fact that 5 ML oxidized Fe shows no remanence. Tracer

experiments with ^{18}O showed that Fe atom transport contributes to the oxidation by at least 80% [22]. This implies a rearrangement of the Fe atoms during the formation of Fe oxide which form epitaxial layers on the substrate prior to oxidation. The disappearance of the LEED image during oxidation suggests a strongly disordered growth of the iron oxide implying the loss of a well defined easy axis within the oxide. It was discussed previously that at higher oxygen exposures formation of the ferrimagnet γ-Fe_2O_3 was found. However, the magnetization of γ-Fe_2O_3 is only 20% of that of bulk Fe and will most likely be further reduced when the oxide is not in a single crystalline phase. Therefore, in the calculation of the non-ferromagnetic layers in figure 6(c) we did not include the contribution of the oxide to the magnetization. The dashed horizontal lines of figure 6(c) indicate film thicknesses of 5 and 8 ML, respectively. From this plot it is obvious that up to 100 L oxygen the decrease of M is independent of the thickness of the Fe films. Above 100 L the progress of oxidation is fastest for the 5 ML film, whereas thicker Fe films on GaAs seem to oxidize much more slowly. Conceivable reasons for this behaviour might be (a) the finite size effect in thin magnetic films, (b) the influence of the surface roughness on the oxidation process or (c) a thickness dependent relaxation of the strained Fe film when oxygen is dosed:

(a) As the Curie temperature is reduced for thinner films the magnetization will also decrease due to this finite size effect when observed at 300 K. Bensch *et al* [23] extrapolated the Curie temperature for Fe/GaAs films as a function of film thickness to 0 K and found a critical thickness for the onset of ferromagnetism at 2.5 ML. The same authors found a steep increase of the Curie temperature with Fe coverage of about 270 K ML^{-1}. Hence this effect cannot be neglected in the case of the 5 and 8 ML Fe film investigated here.
(b) In accordance with [19] we find a gradual sharpening of the LEED images as Fe is continuously deposited on the substrate after diffraction spots can be detected from about 5 ML upwards. It was suggested that growth of Fe takes place in a 3D Volmer–Weber growth mode forming Fe islands which coalesce above 3.5 ML thickness to form a homoepitaxial film on GaAs(001)-(4 × 6). At 5 ML the Fe islands which formed during the initial growth state penetrate the Fe film and give rise to a distinct surface roughness. A further increase of the film thickness will smooth the surface roughness so it possibly becomes better able to passivate the Fe film against further oxidation.
(c) In addition, different strains in the Fe layers can influence the oxidation process.

As discussed previously, a 33 ML Fe film on GaAs(001) showed a decrease of vertical strain from 2.2% to 1.5% after exposure to 1.5 L oxygen. However, for the magnetically characterized film thicknesses from 5 to 16 ML Fe, a thickness dependent relaxation of the oxidized Fe films might also explain the observation that the thicker films oxidize to a lesser extend, since the very thin films are possibly not thick enough to allocate the stress due to the epitaxial growth on GaAs together with the effect of surface oxidation. It should be noted that from a fundamental point of view the oxide formation depends on the partial pressure of oxygen. Although the dosages during our experiments were achieved by varying the oxygen pressure at constant exposure times, we can neglect the pressure dependence, since it was found in [24] that oxides which have been prepared at pressures ranging from 10^{-8} to 10^{-6} mbar with the same coverage lead to the same ratio of 2+ and 3+ ionized Fe atoms (N_{Fe}^{2+}/N_{Fe}^{3+}) as revealed by x-ray photoelectron spectroscopy (XPS).

In the following, the change of magnetic anisotropy due to oxygen adsorption is discussed. The resonance condition for the magnetic field applied parallel to the [1 $\bar{1}$ 0] direction (hard in-plane axis) can be written as [16]

$$\left(\frac{\omega}{\gamma}\right)^2 = \left(B_r^{\parallel} - \frac{2K_4}{M} - \frac{2K_{2\parallel}}{M}\right)\left(B_r^{\parallel} - M_{\text{eff}} + \frac{2K_4}{M}\right). \tag{1}$$

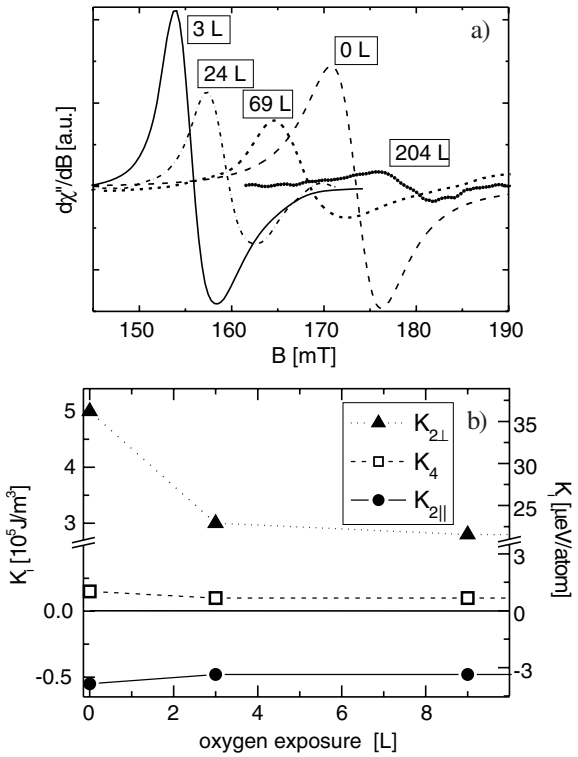

Figure 7. (a) FMR spectra of a 10 ML Fe film at various oxygen exposures measured at 300 K. The magnetic field is applied in the film plane along the [1$\bar{1}$0] direction. (b) Evolution of the anisotropy constants at low oxygen exposures from angle dependent FMR measurements.

Here $B_r^{\parallel}$ is the resonance field and $M_{\text{eff}} = 2K_{2\perp}/M - 4\pi M$ is the effective out-of-plane anisotropy field. Using the magnetization values determined by SQUID it is possible to extract the out-of-plane anisotropy constant $K_{2\perp}$ which describes the intrinsic magnetic anisotropy associated with a rotation of the magnetization between the film normal and film plane. This contribution was found to result mainly from the surface of the Fe films (see [16] for details). $K_{2\parallel}$ denotes the in-plane uniaxial anisotropy constant, describing the magnetic anisotropy between the [110]- and [1$\bar{1}$0] direction. Note that for the Fe/GaAs(001) system the easy axis is given by the [110] direction. K_4 is the fourfold anisotropy constant, resulting mainly from the volume of the film [16] as expected due to the cubic symmetry of Fe. K_4 alone would lead to easy axes along the ⟨100⟩ directions. In contrast to K_4, the uniaxial anisotropy $K_{2\parallel}$ has its origin at the Fe/GaAs-interface [16] and, therefore, for increasing film thickness it becomes less and less important. This leads to a reorientation of the easy axis from the [110] to the ⟨100⟩ direction as function of the film thickness [17]. In our case, however, $K_{2\parallel}$ is still the dominating term for all film thicknesses as already mentioned.

Figure 7(a) shows the derivative of the imaginary part of the high-frequency susceptibility as a function of the external field for oxygen doses between 0 and 204 L. Starting from the clean Fe film with a resonance field of about 1.75 kG, a shift towards lower resonance fields is observed for oxygen doses up to about 10 L. The minimum resonance field was found to be 1.55 kG. Then, for larger doses, the resonance field moves to higher values again, even crossing the resonance field of the clean Fe film. To understand this behaviour we performed

angular dependent measurements of the resonance field at two microwave frequencies for films dosed with 0, 3 and 9 L. From analysis of the complete angular dependence, the anisotropy contributions can be separated. A detailed description of the procedure can be found elsewhere [16]. As can be seen from equation (1), FMR yields, in principle, only the anisotropy fields, i.e. the quantities K_i/M. Within our *in situ* setup, however, the magnetization M is independently measured by the SQUID sensor, so that the anisotropy constants can indeed be derived. The result of the analysis is plotted in figure 7(b), where the various anisotropy constants are given as a function of the oxygen dosage. While almost no change is observed for $K_{2\parallel}$ and K_4 (note that the larger absolute value of $K_{2\parallel}$ indicates the dominance of the uniaxial contribution in the film plane), a reduction of more than 50% of $K_{2\perp}$ can be seen. As found from the SQUID results, almost no change of the sample magnetization is observed for doses up to 10 L. One therefore has to conclude that at the very early stage of oxidation it is mainly the anisotropy of the film that is altered. As the main surface contribution is given by $K_{2\perp}$ it is plausible that this quantity is mostly affected. In an earlier work [16] $K_{2\perp}$ was found to be mainly an anisotropy resulting from the Fe/vacuum interface with only a small volume contribution due to the film strain. As our IV-LEED experiments reveal a relaxation of the film after oxygen dosing, the volume contribution is even smaller than for clean Fe films, thus playing almost no role in the overall value of $K_{2\perp}$.

With M being almost constant at the first stage of oxidation, $K_{2\perp}/M$ is reduced, leading to the negative shift of the resonance field. For higher oxygen doses the change of the anisotropy saturates. As the SQUID data in this case show an increasing reduction of the magnetization, the value of $K_{2\perp}/M$ is increased, leading to the observed shift towards higher resonance fields. Note that the decreasing magnetization is also reflected in the strong reduction of the FMR intensity (area under the integrated FMR signal) as can be clearly seen from the spectra at higher dosage.

4. Conclusion

We performed quantitative measurements of the remanent magnetization of 5–16 ML Fe films on GaAs(001) after exposure steps of oxygen up to 25 000 L at RT. At low oxygen coverage first FeO evolves, which at higher exposures advances to γ-Fe_2O_3.

The 5 ML Fe film loses its remanent magnetization after exposure to only 300 L oxygen, whereas the 8 ML Fe film still conserves remanent magnetization at about 20% of the initial value at 25 000 L. We attribute the reduction of remanent magnetization to the formation of a disordered oxide which is in a spin glass like frustrated state such that no magnetization is measurable in remanence. LEED patterns during oxidation experiments fade away after 6 L of oxygen, indicating a disordered growth of Fe oxide. The progress of oxidation even slows down for the 16 ML Fe film which we attribute to a thickness dependent surface smoothing as checked with LEED prior to oxygen exposure.

At the initial stage of oxidation (up to about 10 L oxygen) the magnetic anisotropy constant $K_{2,\perp}$ is reduced by almost 50% whereas the magnetization remains almost unchanged. After only 1.5 L oxygen exposure the vertical strain of a 33 ML Fe film on GaAs is reduced by almost 30%.

Acknowledgments

This work has been supported by the Deutsche Forschungsgemeinschaft, Sfb 491. We thank R Nünthel for assistance in setting up the IV-LEED system and A Hucht for the analytical calculation of the magnetic stray field.

Appendix

The z-component of the magnetic stray field from a homogenously magnetized square shaped thin film can be expressed analytically as follows:

$$\begin{aligned} B_z(\alpha,\tilde{x},\tilde{y},\tilde{z}) = {} & \frac{3\mu_0\cdot\tilde{z}\cdot M\cdot d}{2\pi L(1-2\tilde{x}+\tilde{x}^2+\tilde{z}^2)(1+2\tilde{x}+\tilde{x}^2+\tilde{z}^2)} \\ & \times\left\{\frac{1}{ABC}\big[-(1-\tilde{y})A\big(\tilde{x}^2(B-C)+(1+\tilde{z}^2)(B-C)-2\tilde{x}(B+C)\big)\cos\alpha\right. \\ & -D(B+C+\tilde{x}(B-C))\sin\alpha\big] \\ & +\frac{1}{EFG}\big[(-1-\tilde{y})E\big(\tilde{x}^2(F-G)+(1+\tilde{z}^2)(F-G)-2\tilde{x}(F+G)\big)\cos\alpha \\ & \left.-D(F+G+\tilde{x}(F-G))\sin\alpha\big]\right\} \end{aligned} \tag{A.1}$$

where

$$\begin{aligned} A &= 1-2\tilde{y}+\tilde{y}^2+\tilde{z}^2 \\ B &= \sqrt{2-2\tilde{x}+\tilde{x}^2-2\tilde{y}+\tilde{y}^2+\tilde{z}^2} \\ C &= \sqrt{2+2\tilde{x}+\tilde{x}^2-2\tilde{y}+\tilde{y}^2+\tilde{z}^2} \\ D &= \tilde{x}^4+2\tilde{x}^2(-1+\tilde{z}^2)+(1+\tilde{z}^2)^2 \\ E &= 1+2\tilde{y}+\tilde{y}^2+\tilde{z}^2 \\ F &= \sqrt{2-2\tilde{x}+\tilde{x}^2+2\tilde{y}+\tilde{y}^2+\tilde{z}^2} \\ G &= \sqrt{2+2\tilde{x}+\tilde{x}^2+2\tilde{y}+\tilde{y}^2+\tilde{z}^2} \\ \tilde{k} &= 2\cdot k/L \quad k=x,y,z. \end{aligned}$$

α denotes the in-plane angle of magnetization with respect to the x-axis, x, y, z are the Cartesian coordinates, $\mu_0 = 4\pi\times 10^{-7}$ V s A^{-1} m^{-1} is the vacuum permeability constant, L is the sample length, M is the sample magnetization and d is the thickness of the film. For our configuration we choose $\alpha = 0$ (scanning direction is parallel to the x-axis) and $y = 0$ since the line scan is performed across the centre of the film. It should be noted that our experimental configuration allows for discrete variation along the y direction in order to find the $y = 0$ position. There, according to the qualitative stray field distribution shown in figure 1 the amplitude of the B_z scan is largest.

The fit of the experimental data as shown in figure 2 requires two parameters, z and M. In the case where M is varied the amplitude of the B_z curve is scaled linearly. Different values of the distance z will alter the amplitude of B_z as well, but in addition will also change the peak positions, i.e. the greater the distance z the farther away are the minimum and maximum positions of B_z.

References

[1] Horgan A M and King D A 1970 *Surf. Sci.* **23** 259
[2] Peng Y, Park C and Laughlin D E 2003 *J. Appl. Phys.* **93** 7957
[3] Schedin F, Hill E W, van der Laan G and Thornton G 2004 *J. Appl. Phys.* **96** 1165
[4] Shima M, Tepper T and Ross C A 2002 *J. Appl. Phys.* **91** 7920
[5] Hodgson A, Wight A and Worthy G 1994 *Surf. Sci.* **319** 119
[6] Grosvenor A P, Kobe B A and McIntyre N S 2005 *Surf. Sci.* **574** 317
[7] Sakisaka Y, Miyano T and Onchi M 1984 *Phys. Rev.* B **30** 8649

[8] Bloński P, Kiejna A and Hafner J 2005 *Surf. Sci.* **590** 88
[9] Simmons G W and Dwyer D J 1975 *Surf. Sci.* **48** 373
[10] Legg K O, Jona F, Jepsen D W and Marcus P M 1977 *Phys. Rev.* B **16** 5271
[11] Salvietti M, Ferro P, Moroni R, Canepa M and Mattera L 1999 *Surf. Sci.* **377–379** 481
[12] Shinjo T, Iwasaki T, Toshihiko T and Takada T 1984 *Japan. J. Appl. Phys.* **23** 283
[13] Getzlaff M, Bansmann J and Schönhense G 1999 *J. Magn. Magn. Mater.* **192** 458
[14] Doi M, Roldan Cuenya B, Keune W, Schmitte T, Nefedov A, Zabel H, Spoddig D, Meckenstock R and Pelzl J 2002 *J. Magn. Magn. Mater.* **240** 407
[15] Ney A, Poulopoulos P, Farle M and Baberschke K 2000 *Phys. Rev.* B **62** 11336
[16] Zakeri Kh, Kebe Th, Lindner J and Farle M 2006 *J. Magn. Magn. Mater.* **299** L1
[17] Gester M, Daboo C, Hicken R J, Gray S J, Ercole A and Bland J A C 1996 *J. Appl. Phys.* **80** 347
[18] Farle M 1998 *Rep. Prog. Phys.* **61** 755
[19] Xu Y B, Kernohan E T M, Freeland D J, Ercole A, Tselepi M and Bland J A C 1998 *Phys. Rev.* B **58** 890
[20] Seo M, Lumsden J B and Staehle R W 1975 *Surf. Sci.* **50** 451
[21] Smentkowski V S and Yates J T 1990 *Surf. Sci.* **232** 113
[22] Leibbrandt G W R, Hoogers G and Habraken F H P M 1992 *Phys. Rev. Lett.* **68** 1947
[23] Bensch F, Garreau G, Moosbühler R, Bayreuther G and Beaurepaire E 2001 *J. Appl. Phys.* **89** 7133
[24] Roosendaal S J, van Asselen B, Elsenaar J W, Vredenberg A M and Habraken F H P M 1999 *Surf. Sci.* **442** 329
[25] Lin W C, Kuo C C, Chiu C L and Li M-T 2001 *Surf. Sci.* **478** 9
[26] Filipe A, Schuhl A and Galtier P 1997 *Appl. Phys. Lett.* **70** 129
[27] Wastlbauer G and Bland J A C 1995 *Adv. Phys.* **54** 137
[28] Wight A, Condon N G, Leibsle F M, Worthy G and Hodgson A 1995 *Surf. Sci.* **331–333** 133
[29] Tepper T and Ross C A 2002 *J. Appl. Phys.* **91** 4453